Frontiers in Bioscience Landmark

Front. Biosci. (Landmark Ed) **2026**; 31(6): 51339
https://doi.org/10.31083/FBL51339

Original Research

Comparative Analysis of Ultra-Low Versus Hydrogel Growing Conditions for Patient-Derived Glioma Organoids

Maria Dudău[1,†], Mugurel Petrinel Radoi[2,3,†], Ionela Daniela Popescu[1], Nicoleta Constantin[1], Valeriu Bogdan Cismasiu[4], Maria Săvoaia[5], Ana-Maria Enciu[1,5,*], Cristiana Tanase[1,6], Elena Codrici[1,5]

[1]Biochemistry-Proteomics Department, Victor Babes National Institute of Pathology, 050096 Bucharest, Romania
[2]Neurovascular Surgery Department, Carol Davila University of Medicine and Pharmacy, 050047 Bucharest, Romania
[3]Department of Vascular Neurosurgery, National Institute of Neurology and Neurovascular Diseases, 077160 Bucharest, Romania
[4]Cell Biology, Neurosciences and Experimental Miology Department, Victor Babes National Institute of Pathology, 050096 Bucharest, Romania
[5]Cellular and Molecular Biology and Histology Department, Carol Davila University of Medicine and Pharmacy, 050047 Bucharest, Romania
[6]Faculty of Medicine, Titu Maiorescu University, 031593 Bucharest, Romania
*Correspondence: ana.enciu@umfcd.ro; ana.enciu@ivb.ro (Ana-Maria Enciu)
[†]These authors contributed equally.

Academic Editor: Nikos Karamanos
Submitted: 28 February 2026 Revised: 1 May 2026 Accepted: 12 May 2026 Published: 22 June 2026

Abstract

Background: Most data related to high-grade glioma and glioblastoma (GBM) 3D models refer to ultra-low/suspension cultivation systems, for several reasons: easy to initiate, high penetrability of treatments, ease of harvesting for downstream analysis. However, the major limitation of these models is the absence of the extracellular matrix, which enables the specific, local invasiveness of these aggressive brain tumors. **Aim**: This study provides a comparison between ultra-low and several extracellular matrix (ECM) and hydrogel culture conditions for various grades of patient-derived glioma organoids, in terms of cell growth, invasiveness, and release of cytokines/chemokines, as a model for downstream analysis of soluble factors. **Materials and Methods**: Patient-derived glioma organoids were initiated in three different conditions: ultra-low attachment(UL), 3D Matrigel, and dextran-based hydrogels. Human endothelial cells were used for tube assay co-cultures and human normal monocyte cell line SC to assess monocyte invasion and interaction with tumor organoids. **Results**: UL conditions supported organoid formation with better growth rate and easy passaging, and reliable detection of secreted cytokines and chemokines, closely mirroring qualitative secretory profiles observed in tumor explants. In contrast, ECM-based systems enabled invasive growth patterns and co-culture assays, but with a restricted immune cell infiltration and with a reduced detectable level of soluble factors. While qualitative cytokine signatures were preserved across culture platforms, substantial quantitative differences were observed, highlighting the influence of matrix composition on measurable outputs. Preliminary data showed that organoid-forming capacity indicated no clear association with Isocitrate Dehydrogenase 1 (IDH1) mutational status in the tested samples. **Conclusion**: Our findings indicate that UL and ECM-based models provide complementary information and recommend a dual-platform cell culture initiation strategy to maximize robustness and translational relevance in patient-derived glioma research.

Keywords: glioma; organoids; 3D cell culture; hydrogel; tumor microenvironment; monocytes; cytokines

1. Introduction

High-grade Isocitrate Dehydrogenase (IDH)-mutant astrocytoma and glioblastoma (IDH wild-type) are incurable malignancies whose therapeutic refractoriness arises from profound intratumoral heterogeneity, reinforced and nuanced recently by novel techniques such as single-cell RNA-sequencing or *in situ* transcriptomics [1]. Understanding mechanisms responsible for such complexity requires reproducible *in vitro* models, such as tumor organoids—microscopic tissue fragments or cell aggregates, grown in controlled environments. A critical factor influencing the fidelity and utility of these tumor organoids is the choice of culture platform. Two widely used approaches are ultra-low (UL) attachment, which promotes spontaneous formation without exogenous extracellular matrix (ECM), and hydrogel-based systems, which embed tumor tissue or cells within a biomimetic 3D matrix.

Ultra-low attachment conditions [2,3] promote organoid formation without a defined extracellular matrix, which may limit the ability to model certain microenvironmental cues. In contrast, hydrogel scaffolds offer a three-dimensional matrix that can recapitulate key aspects of the tumor microenvironment, including hypoxia, extracellular matrix composition, and mechanical properties, thereby influencing gene expression, invasion, and therapeutic response in aggressive brain tumors [4]. Organic hydrogels provide a supportive environment for cell growth by closely replicating the *in vivo* microenvironment, incorporating essential extracellular matrix (ECM) components, growth factors, and hormones. Their

inherent biocompatibility, ability to promote even spatial cell distribution, and low toxicity make them especially advantageous for tissue modeling, supporting physiologically relevant cell behavior and tumor heterogeneity. Importantly, the microscale mechanical properties of these biomaterials, such as structural integrity, stiffness, porosity and interconnectivity, play a crucial role in regulating cellular functions and behavior within the scaffold [5,6]. However, natural hydrogels often suffer from batch-to-batch variability and limited tunability of their mechanical and biochemical properties, which can affect reproducibility and experimental control [7].

The characterization of *in vitro* models provides evidence related to original tumor mimicry, such as preserved histological markers (e.g., glial fibrillary acidic protein, nestin, vimentin), key genetic modifications (e.g., IDH mutation, chromosomal changes), or other features in line with the purpose of the generated model. However, in terms of protein analysis, most data refer to qualitative comparisons. Moreover, only one model is usually selected, but a comparative analysis of various culture systems is essential in order to optimize tumor models for translational research and precision medicine, as differences in matrix composition and physical properties can significantly impact organoid viability, invasiveness, and molecular fidelity to parental tumors.

Rather than addressing specific molecular mechanisms, this study establishes a methodological framework that enables reliable downstream mechanistic and functional investigations in patient-derived glioma models. Accordingly, the analysis focused on soluble factor (cytokine and chemokine) secretion as a functional readout, based on our previous work in this area and their well-documented relevance to glioma pathogenesis [8,9].

2. Materials and Methods

2.1 Patient Samples and Ethical Statement

The use of human brain tissue and peripheral blood samples was coordinated by the Victor Babes National Institute following ethical and technical guidelines on the use of human samples for biomedical research purposes. Patient glioma tissue and peripheral blood samples were collected at the National Institute of Neurology and Neurovascular Diseases (INNBN) after obtaining informed patient consent under a protocol approved by the INNBN Ethics Committee. 12 patient cases (including recurrent cases) from both male and female subjects, aged 28–73 years, were included in this study (Table 1). Anonymization was performed during sample processing and biobanking. Each sample was annotated with the internal code GBM, followed by a consecutively assigned number. At the time of the initiation of the study, IDH1 status was unknown and the initial diagnosis was based on clinical data and histopathology findings.

2.2 Glioma Initiation Protocol

Initiation of patient-derived glioma organoids was performed as described in Gamboa et al. [10]. Patient-derived samples were processed under sterile conditions using a laminar flow hood with cold 1× PBS and antibiotics. The samples were minced, then digested with 2 mL of Accutase at 37 °C. Following digestion, they were filtered through a 40 µm cell strainer and washed with 10 mL of cold PBS. The sample was then centrifuged at 800 × g for 2 minutes at 4 °C. After centrifugation, red blood cell lysis buffer was added to the resuspended pellet for 5 minutes at room temperature. After red blood cell lysis, 25 mL of 1× PBS is added and the sample is centrifuged as before. The final pellet was resuspended in complete culture medium (EMEM w/glutamine, supplemented with Primocin 100 µg/mL, EGF and bFGF 20 ng/mL each, B27 1× and hydrocortisone 50 ng/mL and ROCK1/2 inhibitor 10 µM 1×). Primocin and ROCK inhibitors were added to the medium only after initiation/derivation of tissue, not in the basal medium. Medium was prepared fresh twice a week. All cell cultures used in this study were tested negative for mycoplasma.

2.3 Culture Conditions

The cellular pellet was split into three parts and used for different culture conditions: 96-well ultra-low attachment plates: cells were resuspended in 200 µL complete medium per well × number of wells to seed; Matrigel Organoid (Corning, 356255): 35 µL Matrigel and cells in complete medium at a 4:1 (v/v) ratio per well; 35 µL dextran-based hydrogel and cells, prepared according to the manufacturer's instructions (TrueGel3D Hydrogel Kit-True7-1kt, Merck).

2.4 Tissue Explants

Small (1–2 mm^3) tumor tissue fragments were incubated in ultra-low conditions in complete cell medium, on continuous shaking, at 37 °C and 5% CO_2 atmosphere. Before medium replenish, supernatant was sampled, aliquoted and stored at –80 °C for cytokine analysis.

2.5 Cell Line Cultures and Cell Treatments

The human endothelial cell line EA.hy926 (P8) (CRL2922, ATCC, VI, USA) and human monocyte cell line SC (P12) (CRL9855, ATCC, VI, USA) were routinely maintained in a cell incubator at 37°C in a humidified atmosphere containing 5% CO_2, in the media formulations recommended by the manufacturer.

Endothelial cells were nucleofected with plasmid green fluorescence protein - pGFP (Lonza Nucleofector system, program EO-100, Nucleofector Solution set SE, PBC1-02250). For tube formation assay, 35,000 endothelial cells were plated in 25% Matrigel with DMEM supplemented with 10% FBS and 20 ng/mL EGF.

Table 1. Patient data.

Code	Gender/age (years)	Tumor location	Histopathology
GBM1	Male/66	Tumoral necrosis, temporal	Glioblastoma (small cells, monomorphic)
GBM2	Male/61	Parietal, infiltrative	Glioblastoma
GBM3	Male/73	Parietal, infiltrative	Glioblastoma (macrophagic reaction)
GBM4	Female/73	Temporal, infiltrative	Glioblastoma
GBM5	Male/46	Temporal, recurrent	Glioblastoma
GBM6	Female/66	Temporal, infiltrative	Glioblastoma
GBM7	Female/52	Temporal and parietal, infiltrative, necrosis	Glioblastoma
GBM8	Male/32	Necrosis, frontal	Glioblastoma
GBM9	Male/50	Temporal, necrosis	Glioblastoma
GBM10	Male/28	Recurrent	Astrocytoma, differentiated, grade 3
GBM11	Male/73	Frontal, necrosis	Glioblastoma
GBM12	Male/39	Temporal, infiltrative, recurrent	Diffuse Astrocytoma

Monocytes were nucleofected with pGFP (Lonza Nucleofector- EA-100, P3 Nucleofection solution, 4D-Nucleofector X Optimization kit for primary cells, V4XP-9096, Lonza, Basel, Switzerland).

2.6 Immunofluorescence

Organoids were washed twice with PBS and fixed with 4% paraformaldehyde solution for 30 minutes at 37 °C. Following fixation, organoids were washed with 0.1% Triton X-100 in Tris-buffered saline (TBS-Tx) at RT. Permeabilization was performed using 5% BSA and 2% Triton X-100 in PBS for 2 hours at RT. After permeabilization, blocking was carried out using 2% BSA in PBS for 1 hour at RT. For primary immunostaining, the cells were incubated at 4 °C for 24 hours with the primary antibodies: anti-vimentin monoclonal antibody, (MA5-11883, Invitrogen, MA, USA) ; anti-nestin antibody 10C2, (MA1-110, Invitrogen, MA, USA); anti-glial fibrillary acidic protein - GFAP D1F4Q XP Rabbit monoclonal antibody, (Cell Signaling Technology, 12389S), diluted 1:100 in blocking solution (2% BSA in PBS). Next, the cells were washed three times for 5 minutes with 0.1% TBS-Tx. For secondary immunostaining, the cells were incubated at room temperature for 3 hours with the secondary antibodies: Alexa Fluor 568 goat anti-mouse IgG H+L, (Invitrogen, A11004); Alexa Fluor 488 goat anti-rabbit IgG H+L, (Invitrogen, A11008) diluted 1:1000 in PBS. The nuclei were counterstained using DRAQ5 diluted 1:1000 in PBS (ab108410, Abcam, Cambridge, UK).

Frozen tissue was embedded in OCT compound and sectioned in a cryostat at –20 °C. Cryosections were additionally fixed for 10 minutes in cold acetone: methanol solution (1:1 v/v), permeabilized for 10 minutes in 0.1% Triton X-100 in 0.5% BSA in PBS, then blocked and antibody incubation as previously described. Image acquisition was performed using Leica TCS SP8 STED microscope for tissue sections and Operetta CLS (Revvity, Boston, MA, USA) high-content imaging system for organoids.

2.7 Western Blot

Organoids were lysed in 500 µL RIPA buffer with 1% protease inhibitor cocktail (P2714, Sigma, MI, USA) and 30 µg total proteins were separated by SDS-PAGE in 10% acrylamide gel, at 20 mA/gel for 2 h. Transfer of proteins onto nitrocellulose membranes was performed on ice at 100 V for 1 h. Blotting membranes were incubated for 1 h in 5% BSA/TBS-T, then o/n in primary antibodies 1:1000: anti-GFAP D1F4Q XP Rabbit monoclonal antibody (12389S, Cell Signaling Technology, MA, USA), anti-vimentin monoclonal antibody (MA5-11883, Invitrogen, MA, USA), anti-nestin monoclonal antibody 10C2 (MA1-110, Invitrogen, CA, USA), anti-O6-methylguanine-DNA methyltransferase -MGMT antibody MT 3.1, sc56157 (Santa Cruz Biotechnology, CA, USA), anti glyceraldehyde-3-phosphate dehydrogenase rabbit polyclonal antibody 1:4000 - GAPDH (PA1-987). On the second day, membranes were washed 3 times in TBS-Tween20 0.1% and 1 time in TBS, 10 min each wash, then incubated for 1 h at RT in HRP-conjugated secondary antibodies, 1:40,000 (goat-anti rabbit, Licor, 926-80011 and goat-anti mouse Licor, 926-80010, LI-COR Biosciences, NE, USA). After incubation, membranes were washed the same as before and incubated for 5 minutes in ECL solution (1705062, BioRad, CA, USA). Image acquisition was performed with the c-DIGIT blot scanner (LI-COR Biosciences, NE, USA).

2.8 DNA Isolation and RNase H2 Dependent PCR (RH-PCR)

Frozen tissues (5–15 mg) and cultured cells were used for DNA isolation. DNA was extracted with PureLink Genomic DNA Mini Kit (K1820, Thermo Fisher Scientific, CA, USA). Quantification of DNA samples was performed with a NanoDrop 2000 Spectrophotometer (Thermo Fisher Scientific, CA, USA). The PCR reactions were prepared as a mixture of GoTaq qPCR Master Mix (A6001, Promega, WI, USA), custom rhPrimer GEN1 (Integrated DNA Technologies, USA) and RNase H2 Enzyme Kit (11-

02-12-01, Integrated DNA Technologies, USA). In this assay, each primer contains a single ribonucleotide residue and a 3′ blocking moiety [11]. PCR amplification is initiated by the *Pyrococcus abyssi* RNase H2 enzyme, which cleaves at the ribonucleotide site, removing the blocking group and generating an extendable primer. The ribonucleotide is positioned within the primer sequence corresponding to the mutation or SNP site. Since cleavage occurs only when the ribonucleotide-containing primer perfectly matches the target sequence, amplification is highly specific to the intended SNP or mutation. The reaction mixture contained 7.5 µL of the supplied 2X master mix, 0.5 µL of each primer (0.3 µM final concentration each), 1 µL diluted RNase H2 (2.6 mU) and 5.5 µL of the template (5 ng genomic DNA). The cycling conditions were as follows: denaturation for 10 min at 95 °C, amplification for 40 cycles, with denaturation for 10 sec at 95 °C, annealing, ribose digestion, and primer extension for 60 sec at 66 °C. The assays were run on the QuantStudio 7 Flex equipped with a Fast 96-well block and analysis was performed using the software QuantStudio PCR v3.1 (Thermo Fisher Scientific, CA, USA). The primer sequences are as follows: primer forward 5′-ggaaatcaccaaatggcaccatacg-3′; primer reverse specific for IDH wt 5′-gacttacttgatccccataagcatgacgaccAx-3′ and the one specific for mutant IDH1 R132H is 5′-gacttacttgatccccataagcatgatgaccAx-3′ (ribose is underlined and X = C3 spacer).

2.9 Cytokine Quantification

Cytokine levels in the culture medium were quantified using a multiplex bead-based immunoassay (Milliplex MAP Human Cytokine/Chemokine Magnetic Bead Panel 12-plex, HCYTOMAG-60k, Merck Millipore, Burlington, MA, USA), according to the manufacturer's instructions. The assay targets included G-CSF, IFN-γ, IL-10, IL-12p70, IL-1β, IL-2, IL-6, IL-7, IP-10, MCP-1, MIP-1α, and TNF-α. Each analyte had a 7-point dilution curve for sample quantification. Beads were incubated with assay buffer, cytokine standards, or samples in 96-well plates overnight at 4 °C under orbital shaking (800 rpm). Detection involved incubation with biotinylated antibodies and Streptavidin-Phycoerythrin (SAPE) in the dark at room temperature. Data acquisition was performed using the Luminex 200 system (Luminex Corp., Austin, TX, USA) , and the results were analyzed with xPONENT 4.2 software (Luminex Corp., Austin, TX, USA), utilizing a five-parameter logistic standard curve. All samples were analyzed in duplicate, and mean values were used for further interpretation.

2.10 Protein Quantification

The supernatant collected for cytokine analysis was also used to quantify total protein content using the Pierce BCA Protein Assay Kit (Cat. No. 23225, Thermo Fisher Scientific, CA, USA) following the manufacturer's instructions. The protein concentration was used to normalize the multiplex cytokine data.

2.11 Statistical Analysis

Statistical analysis was performed using GraphPad Prism 7 (GraphPad Software, Boston, MA, USA). Data are presented as mean ± SD. Monocyte infiltration data are shown as the mean of three determinations ± SD and a two-tailed unpaired *t*-test was used for analysis. Cytokine values were measured in duplicate, and normalized to total protein content. Due to the limited sample size and exploratory nature of the study, results were interpreted descriptively, without formal *p*-value-based significance testing. Experiments were performed in duplicates or triplicates for each biological sample.

3. Results

3.1 The Behavior of Tumor Cells in Various 3D Culture Conditions Differs Between Glioma Samples and Does Not Correlate With IDH1 Status

Glioma biopsies were grown under three different conditions: suspension cell culture (96-well ultra-low attachment plates) or hydrogels – organic (Matrigel Organoid, Corning) and dextran-based with cross-linker (T7, Merck, MA, USA). For the latter, our previous tests on cell lines [12] showed that RGD (a peptide that mediates cell adhesion) favored spreading of cells, preventing the formation of organoids; therefore, it was not added to the mix.

Analysis of different glioma samples showed that not all cells have the same ability to form organoids in ultra-low wells, nor can they infiltrate or form spheres in hydrogels. While some samples, like GBM5 and GBM7, would generate organoids within the first 7 days of cultivation, or during subsequent passaging and could be propagated for four passages, other samples required more than 21 days (e.g., GBM9) or did not form organoids in any of the tested conditions (GBM8) (Fig. 1A). In addition, some samples showed an infiltrative behavior in hydrogels, even though dextran-based hydrogel is a restrictive environment (**Supplementary Fig. 1**). Organoid growth was optimal in ultra-low attachment plates for all tested samples, despite sample-to-sample variation, and facilitated passage. By contrast, in semi-solid media, growth was slower and some of the cultures could not be propagated after passage 1. Immunophenotypic validation confirmed that key biomarkers identified in the primary tumor by Western blot (WB) and/or immunofluorescence (IF) (specifically vimentin, nestin and GFAP) remained positive within the derived glioma organoids (Fig. 1B–D). Culture initiation, passage, and downstream analysis are summarized in Table 2. For GBM9-12, 2D initiation was not considered an option, as ultra-low derivation was always successful.

The next question to be addressed was whether the IDH1 status was correlated with the ability to form organoids. Of the tested glioma samples, GBM8, which failed to form organoids in UL or hydrogels, was shown to be positive for the R132H mutation, but with a very low

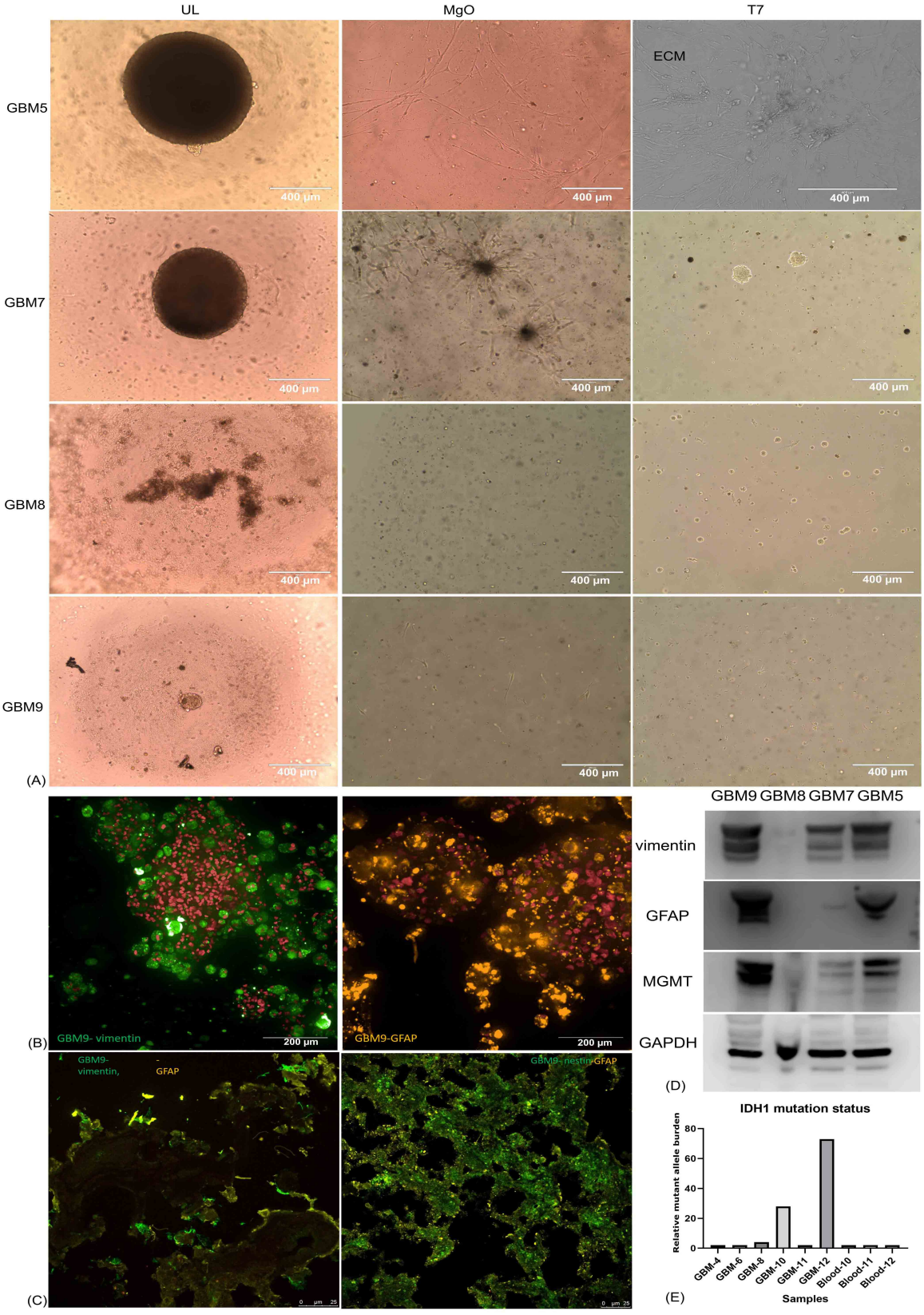

Fig. 1. Assessment of primary glioma samples. (A) Different types of behavior of glioma samples in ultra-low attachment (UL) and hydrogel conditions (Matrigel Organoid and dextran-based T7 hydrogel). Phase-contrast microscopy 10×. (B) Immunofluorescence assessment of tumor biomarkers was investigated in patient-derived organoids grown in ultra-low and comparatively detected in frozen tissue section by immunofluorescence (C) and Western blot (D). (E) IDH1 R132H mutation burden was assessed by rhPCR. Scale bars: (A) 400 µm; (B) 200 µm; (C) 25 µm. GFAP, glial fibrillary acidic protein; MGMT, methylguanine-DNA methyltransferase.

Table 2. Culture type, passaging and downstream analysis for PDGOs.

Sample	2D/Explant			UL			MgO			Hydrogel			IDH testing	Cytokine assay	IF
	Initiation	Passage	Time in culture	Initiation	Passage	Time in culture	Initiation	Passage	Time in culture	Initiation	Passage	Time in culture			
GBM1	No	No	-	Yes	No	17 days	Yes	No	17 days	No	No	-	No	No	No
GBM2	Yes	Yes-2	28 days	No	No	-	No	No	-	No	No	-	No	No	Yes
GBM3	No	No	-	No	No	-	Yes	No	7 days	No	No	-	No	No	No
GBM4	Yes	Yes-2	21 days	No	No	-	No	No	-	No	No	-	WT	No	Yes
GBM5	Yes	No	14 days	Yes	Yes-3	>3 mo.	Yes	Yes-1	2 mo.	Yes	Yes-1	6 w.	WT	Yes	Yes
GBM6	No	No	-	Yes	Yes-1	2 mo.	Yes	Yes-1	2 mo.	Yes	Yes-1	6 w.	WT	Yes	Yes
GBM7	No	No	-	Yes	Yes-4	>3 mo.	Yes	Yes-4	>3 mo.	Yes	Yes-3	>3 mo.	WT	Yes	Yes
GBM8	Yes	No	10 days	Yes	Yes	>3 mo.	Yes	Yes-2	>3 mo.	Yes	Yes-1	6 w.	R132H	Yes	Yes
GBM9	No	No	-	Yes	Yes	2 mo. 1 w.	Yes	Yes-3	>3 mo.	Yes	Yes-2	2 mo.	WT	Yes	Yes
GBM10	No	No	-	Yes	Yes-1	>3 mo.	Yes	Yes-1	2 mo.	Yes	No	-	R132H	Yes	Yes
GBM11	No	No	-	Yes	Yes-1	>3 mo.	Yes	Yes-1	2 mo.	Yes	No	-	WT	Yes	Yes
GBM12	No	No	-	Yes	Yes	>3 mo.	Yes	Yes-1	2 mo.	Yes	No	-	R132H	Yes	Yes

mo., months; w., week; PDGOs, patient-derived glioma organoids; IDH, Isocitrate Dehydrogenase.

burden. In order to confirm whether lower-grade gliomas form organoids in ultra-low wells or not, we investigated the behavior of two more samples of relapsed IDH1 R132H-positive astrocytoma (GBM10, GBM12). After 21 days, GBM10 only formed small cellular aggregates, while GBM12 quickly formed organoids at passage 0 and passage 1. Of note, although the initial diagnosis of the tumor was diffuse astrocytoma, the histopathological diagnosis of the GBM12 relapse was glioblastoma, based on pathological assessment of aggressive features characteristic of this stage. When quantified, IDH1 mutational burden was higher in GBM12 than in GBM10, showing that IDH1 R132H mutation is not a criterion to explain the different behavior of samples in ultra-low conditions (Fig. 1E).

3.2 Extracellular Matrix Allows Co-Cultivation Assays, While Providing the Necessary Scaffold for Cellular Networks

Our next step was to determine whether adding a second cell type to the cultivation model could drive organoid development. By using hydrogels, we were able to directly co-culture tumor cells with endothelial cells. This approach involved first developing an endothelial tube-formation assay and then seeding it with glioma cells. Endothelial cells were GFP-transfected, allowed to form tubes for 48 hours, and then glioma cells were added. As shown in Fig. 2A, after 60 hours of incubation, glioma cells, rather than scattering into the hydrogel, were aligned with the endothelial networks.

The choice of cultivation medium also influenced monocyte behavior; hydrogel-based cultivation resulted in a 'cold' model with monocytes being largely restricted to the hydrogel surface or the periphery of the infiltrative margins (Fig. 2B, **Supplementary Movie 1**). Monocyte infiltration was quantified by comparing the fluorescence signals between intra-tumoral and extra-tumoral regions (Fig. 2C). However, in ultra-low wells, monocytes rapidly infiltrated the organoids in as little as 6 hours and were still visible at 24h (Fig. 2D).

3.3 For Cytokine Expression, Ultra-Low Conditions Are the Best Option to Study Secretory Profile of Tumor Cells

The soluble cytokine profile was compared in tissue explants and organoids grown in different culture conditions for two IDH1 wild-type samples and two IDH1 R132H mutated samples. Of the tested cytokines, MCP-1 was expressed at high levels in most conditions (Fig. 3A–D). When compared to tissue, ultra-low-grown samples showed a comparable expression trend for MCP-1 and consistently allowed for the detection of IP-10, if present in the tissue. In turn, MIP-1a was induced/increased in ultra-low concentrations when compared to tissue samples.

Other low-level inflammatory cytokines, IL-6 (Fig. 3E) and TNFα (Fig. 3F), if quantifiable in tissue samples, were also detectable in ultra-low conditions. Although cytokine levels were lower in the ultra-low samples, the tumor cell types within the organoids represented the sole source of these cytokines, which is a key difference from the tissue samples.

To test the dependence of MCP-1 expression on culture conditions, two GBM wild-type samples, which allowed initiation of a 2D cell culture, with and without laminin-based extracellular matrix (ECM), were analyzed in terms of secreted proteins (Fig. 3G). MCP-1 showed consistent expression when cells were grown in 2D (with or without organic extracellular matrix), but 3D culture conditions caused substantial changes.

As a summarizing observation, the usage of semisolid culture matrices lowers the amount of secreted cytokines, which can hinder detection in case of a low-expression protein.

4. Discussion

The aim of this study was to identify a three-dimensional glioma model that best recapitulates *in vivo* tumor architecture and microenvironmental complexity, thereby providing physiologically relevant insight into cell-to-cell interactions and cytokine production. Ultra-low growth conditions provide an easy-to-use and reproducible model, which, as previously demonstrated, recapitulates the features of the original tumor [2]. Other advantages of ultra-low systems are ease of passaging and periodic sampling of soluble molecules enriched in the cell culture supernatant, as well as reduced costs, and minimal technical complexity.

The need for a different type of culture, beyond ultra-low, was the assessment of stroma-to-tumor cell-to-cell interactions. Conditioning media models or simultaneous ultra-low co-cultivation of two cell types in suspension is less informative than an ECM-based model; therefore, a two-step model was tested: first, an endothelial network was established in ECM using GFP-transfected cells, then glioma cells were incubated and image acquisition was performed daily. Previous data by McCoy et al. [13] showed that the presence of matrix-embedded endothelial cells increases the invasiveness of glioma cells. Our model also supports this finding, albeit starting from isolated cells, not fully formed organoids. A novel observation provided here was that after 60 hours of co-cultivation, primary glioma cells started to organize according to the previously lattice-like established architecture, rather than forming infiltrating organoids.

Regarding immune-to-tumor cell interactions, the presence of ECM impeded the infiltration of GFP-monocytes. Previous data stated that 3D cultivation of GBM cells biases toward cytokine secretion and macrophage recruitment by upregulation of soluble cytokines and chemokines [14]. The relevance of this argument could be further studied in a hydrogel-based infiltrative tumor model, such as the one provided here.

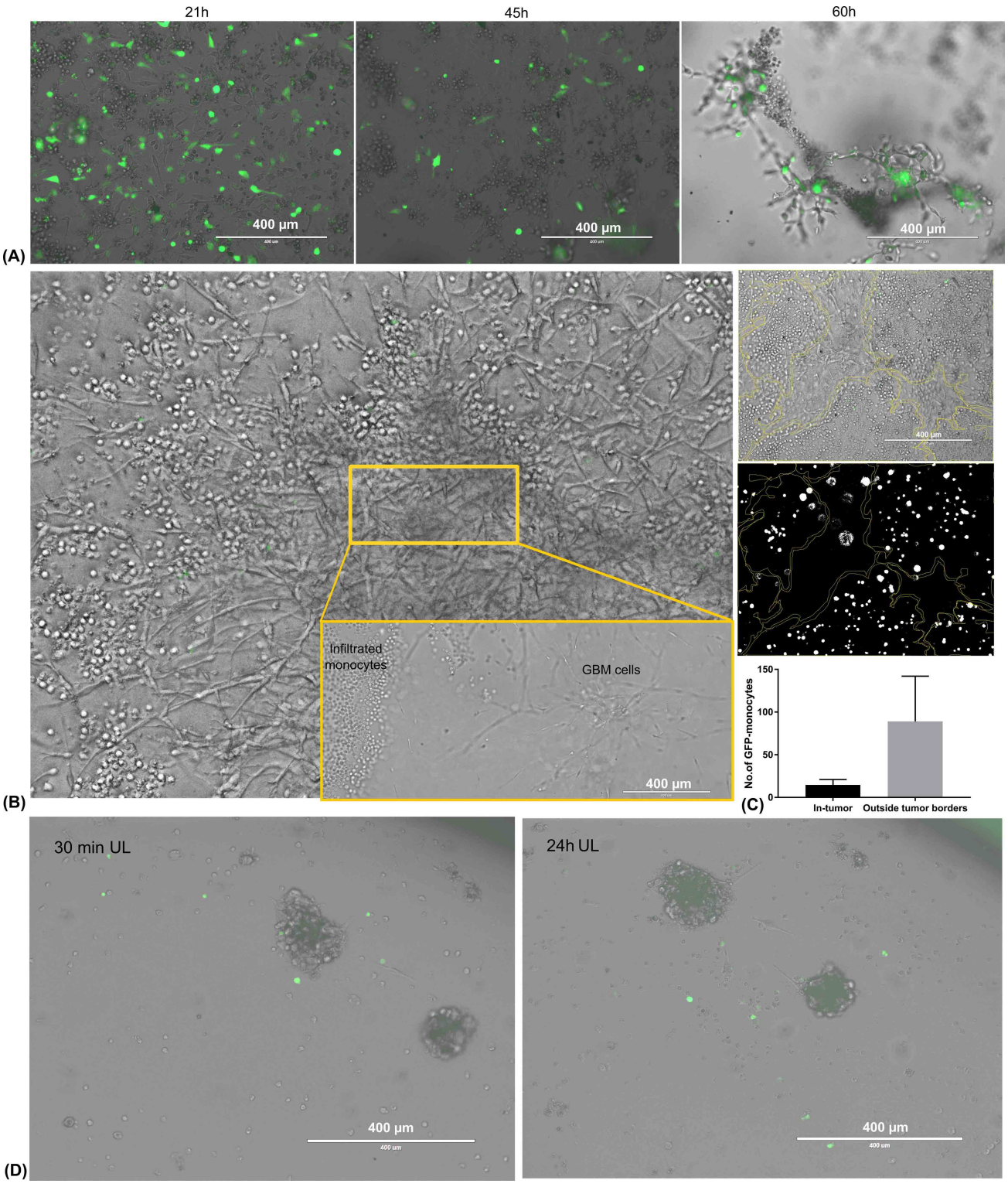

Fig. 2. Co-cultivation models of glioma organoids. (A) Co-cultivation of glioma cells into previously grown endothelial networks. GFP-EaHy cells were allowed to form networks in Matrigel, then incubated with glioma cells (untransfected). Phase-contrast microscopy 10×. (B) Matrigel-grown glioma patient-derived cells were incubated with monocytes. The image is a composite result of a Z-stack scan, while the insert is a detail of one of the planes. (C) Analysis of GFP-monocytes infiltration between intra-tumoral and extra-tumoral regions was assessed by quantification of fluorescent signals. Bars represent the average of three determinations ± SD. Two-tailed unpaired *t*-test showed no statistical significance ($p > 0.05$). (D) Patient-derived glioma organoids grown in ultra-low (UL) wells were incubated with GFP-monocytes. Scale bar, 400 µm.

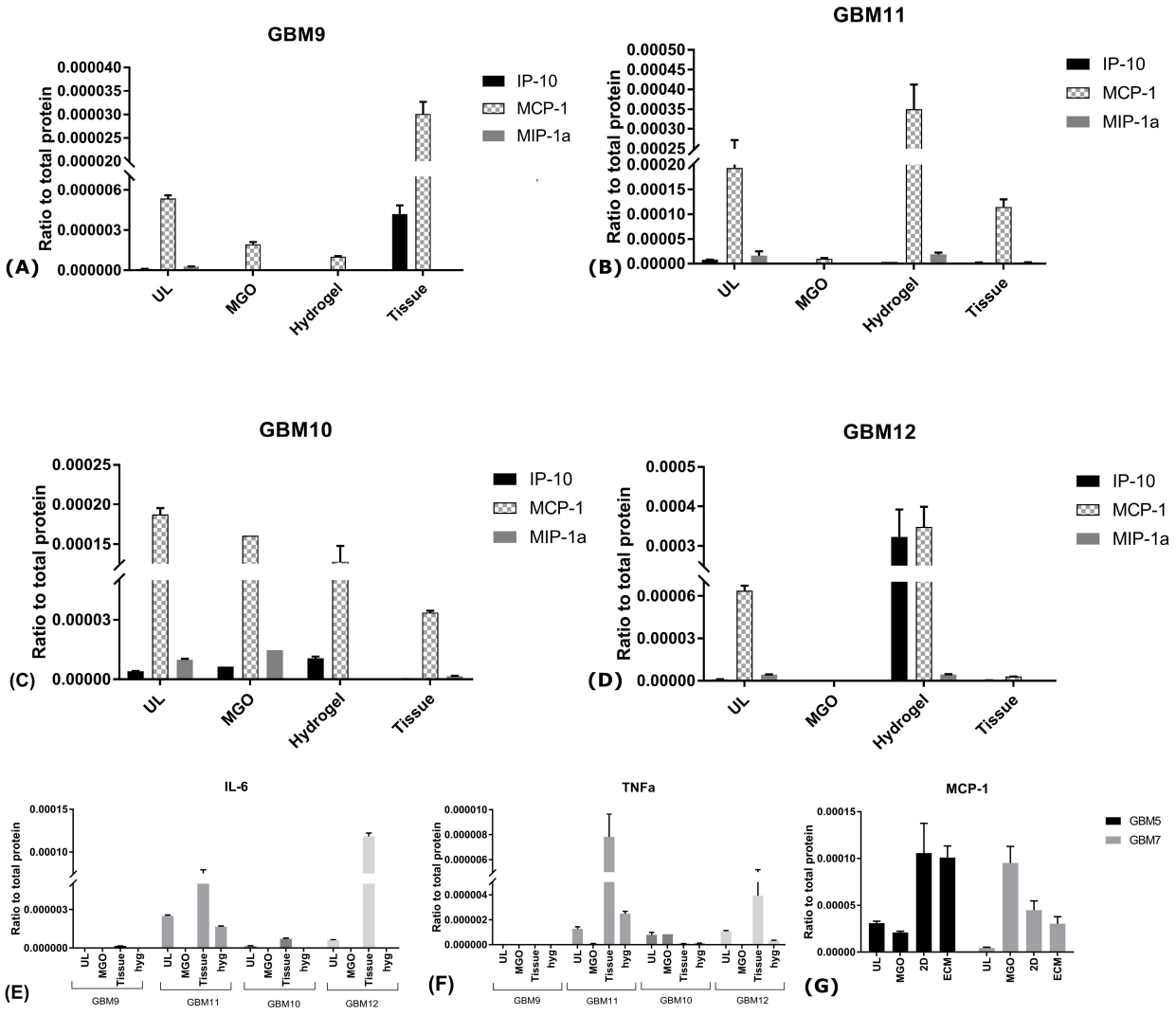

Fig. 3. Comparison of cytokine expression. Comparison of relative cytokine expression between different types of cell culture and tumor tissue for two WT GBM (GBM9 and GBM11) and two IDH1 R132H mutated gliomas (GBM10 and GBM12) for highly expressed cytokines (A–D) and low expression cytokines (E,F). Lower levels of cytokines are typically detected in the supernatant of organoids grown in organic Matrigel (MgO) compared to other culture conditions. (G) 2D cultures w or w/o ECM coating show consistent expression of abundant proteins, but 3D culture conditions can induce changes. The absolute value of cytokine expression was normalized to total protein content. Bars represent the average of duplicates ± S.D.

Finally, we analyzed the cytokine profile across the three cultivation platforms: ultra-low attachment wells, Matrigel, and dextran-based hydrogels. Given that tumor-immune cell communication relies on soluble signals, we sought to determine how each matrix influenced the cytokine and chemokine landscape. A study by Park et al. [15] analyzed five different cultivation platforms, employing collagen and patient-derived, decellularized ECM, from both normal and tumor tissue and argued that suspension cell culture method best preserved the transcriptional profile of the tumor tissue. Other suspension protocols also report consistency between the histologic and genomic landscape of the tissue of origin and derivative organoids [15,16].

Our study also demonstrates consistency between the tissue explants' secretory profile and the three tested *in vitro* conditions. However, while the qualitative protein signature was preserved, quantitative expression levels varied. Notably, proteins undetectable in the tumor tissue remained absent *in vitro*, indicating that none of the culture conditions significantly altered the fundamental protein composition of the panel. However, in terms of quantification, we were able to consistently observe increased levels of monocyte chemotaxis protein (MCP-1) in *in vitro* samples, as opposed to tumor tissue. MCP-1 was reported to be produced by glioblastoma cells and involved in invasion and migration [17], as well as generation of an immunosuppressive environment. This can be explained by the enrichment

of MCP-1-producing cells in our setup. The absolute variations noted between cultivation methods (ultra-low, Matrigel Organoid or dextran-based hydrogel) could arise from at least two sources: the cell number actively producing the secretory proteins, or the existence of ECM-related signals able to modify protein expression. ECM is a limiting factor in terms of cellular expansion and, for some samples, small organoids could be visualized in UL, but not formed in ECM, regardless of the cultivation time. As a consequence, higher levels of MCP-1 protein were detected in UL when compared to Matrigel Organoid. This finding was not, however, extended to dextran-based hydrogel, possibly due to different ECM composition. It has been known that some cytokines interact with ECM molecules such as the negatively-charged glycosaminoglycans [18], thus preventing their release in the cell supernatant. Specifically, heparin has long been proposed as an adsorptive pro-inflammatory cytokine substrate [19]. In contrast, non-sulphated dextran is a neutral molecule, with little interaction with cytokines, allowing their release in the cellular supernatant, hence the different profile of cytokine release between two different semisolid media.

Finally, another observation is that multiple seeding methods from the same tumor might increase the success rate of culture initiation. This rate is usually higher (around 60%) for ultra-low/hanging droplet method [20] than for Matrigel/hydrogel methods (less than 50%) [21] and our experience also supports this finding. In order to increase the chances of success in obtaining primary 3D tumor organoids, a dual initiation (UL and semisolid gels) is recommended. However, choosing a basement membrane-like gel composition creates a tumor environment more similar to *in vivo* conditions. ECM entrapment is a physiological mechanism by which cells limit the diffusion of soluble molecules and control extracellular cues.

5. Limitations

This study is limited by the small cohort size and the biological heterogeneity of the sample set, which may reduce the clinical relevance of the study. In addition, the co-culture experiments were performed using established monocyte cell lines rather than patient-matched primary cells, thereby limiting physiological relevance. For 3D cultures, normalization of quantifiable biomarkers is still challenging, especially since larger organoids are known to develop a necrotic core [22], which implies that normalization to organoid size induces its own bias. Finally, the quantitative comparison of secreted factors across matrices should be interpreted with caution, as extracellular matrices may influence cytokine diffusion, retention, or recovery independently of true cellular secretion.

6. Conclusions

This study aimed to identify an optimum *in vitro* 3D model for patient-derived glioma samples, which would support imaging investigation and reliable assessment of protein profiles related to the tissue of origin. Although ultra-low cultivation and several types of ECM provide satisfactory results, an integrated analysis requires at least two simultaneous models. The ultra-low method combined with organoid Matrigel model offers multiple complementary pieces of information and it is recommended to be implemented as a routine initiation method.

Availability of Data and Materials

The datasets used and analyzed during the current study are available from the corresponding author on reasonable request.

Author Contributions

AME, CT, EC designed the research study; MPR provided the initial clinical diagnosis of the patients, the samples and follow-up data; MD, AME, NC, performed cell cultures initiation and maintenance; MS optimized and performed IF experiments; VBC designed primers, optimized and performed PCR; AME performed WB; IDP and EC performed multiplex assay. AME, VBC and CE analysed the data. MD and AME wrote the initial draft of the article. All authors contributed to editorial changes in the manuscript. All authors read and approved the final manuscript. All authors have participated sufficiently in the work and agreed to be accountable for all aspects of the work.

Ethics Approval and Consent to Participate

The study was conducted in accordance with the Declaration of Helsinki. Patient glioblastoma tissue and peripheral blood samples were collected at the National Institute of Neurology and Neurovascular Diseases (INNBN) (Approval no.12211/23.11.2023) after informed patient consent under a protocol approved by the INNBN Ethics Committee. Each patient provided signed informed consent, specifically agreeing to the use of collected biological samples for research and publication purposes.

Acknowledgment

We thank Dr. Emanuel Fertig for the immunofluorescence tissue image acquisition and Cromatec S.A. for in-kind access to HCS Operetta CSL. We would like to acknowledge the contribution of CA21135 - Modelling immunotherapy response and toxicity in cancer (IMMUNOmodel), which, through its conferences, workshops and webinars, brought a better understanding of immune-to-tumour cell interactions. Also, we would like to thank Dr. Igor Pongrac and Dr. Andrei Tanase from Merck Discovery for their technical and scientific support. The authors acknowledge professional language editing, proofreading, and revision support for the manuscript provided by Irina Bratu (credentials: E0048/2014, Medicine-Pharmacy).

Funding

This research was funded by Core Program within the National Research, Development and Innovation Plan, 2022–2027, with the support of MCID, project no. 10N/01.01.2023, PN 23.16.01.01; PN 23.16.02.03.

Conflicts of Interest

The authors declare no conflicts of interest.

Declaration of AI and AI-Assisted Technologies in the Writing Process

During the preparation of this work, Gemini AI and ChatGPT were used solely for the purpose of rephrasing and English proofing of limited paragraphs. After using these tools, the authors reviewed and edited the content as needed and take full responsibility for the content of the publication. No images, data analysis or other graphical data were generated using AI.

Supplementary Material

Supplementary material associated with this article can be found, in the online version, at https://doi.org/10.31083/FBL51339.

References

[1] Greenwald AC, Darnell NG, Hoefflin R, Simkin D, Mount CW, Gonzalez Castro LN, et al. Integrative spatial analysis reveals a multi-layered organization of glioblastoma. Cell. 2024; 187: 2485–2501.e26. https://doi.org/10.1016/j.cell.2024.03.029

[2] Jacob F, Salinas RD, Zhang DY, Nguyen PTT, Schnoll JG, Wong SZH, et al. A Patient-Derived Glioblastoma Organoid Model and Biobank Recapitulates Inter- and Intra-tumoral Heterogeneity. Cell. 2020; 180: 188–204.e22. https://doi.org/10.1016/j.cell.2019.11.036

[3] Park J, Kim D, Park HC, Park M, Zhang S, Na O, et al. Tumor microenvironment-preserving gliosarcoma organoids as an in vitro preclinical platform: a comparative analysis with glioblastoma models. Journal of Translational Medicine. 2025; 23: 915. https://doi.org/10.1186/s12967-025-06952-y

[4] Chen JWE, Pedron S, Harley BAC. The Combined Influence of Hydrogel Stiffness and Matrix-Bound Hyaluronic Acid Content on Glioblastoma Invasion. Macromolecular Bioscience. 2017; 17: 10.1002/mabi.201700018. https://doi.org/10.1002/mabi.201700018

[5] Ruiz-Garcia H, Alvarado-Estrada K, Schiapparelli P, Quinones-Hinojosa A, Trifiletti DM. Engineering Three-Dimensional Tumor Models to Study Glioma Cancer Stem Cells and Tumor Microenvironment. Frontiers in Cellular Neuroscience. 2020; 14: 558381. https://doi.org/10.3389/fncel.2020.558381

[6] Del Rocío Aguilera-Marquez J, Manzanares-Guzmán A, García-Uriostegui L, Canales-Aguirre AA, Camacho-Villegas TA, Lugo-Fabres PH. Alginate-Gelatin Hydrogel Scaffold Model for Hypoxia Induction in Glioblastoma Embedded Spheroids. Gels (Basel, Switzerland). 2025; 11: 263. https://doi.org/10.3390/gels11040263

[7] Liang L, Cui R, Zhong S, Wang Z, He Z, Duan H, et al. Analysis of the potential role of photocurable hydrogel in patient-derived glioblastoma organoid culture through RNA sequencing. Biomaterials Science. 2022; 10:4902–4914. https://doi.org/10.1039/d2bm00589a

[8] Birocchi F, Cusimano M, Rossari F, Beretta S, Rancoita PMV, Ranghetti A, et al. Targeted inducible delivery of immunoactivating cytokines reprograms glioblastoma microenvironment and inhibits growth in mouse models. Science Translational Medicine. 2022; 14: eabl4106. https://doi.org/10.1126/scitranslmed.abl4106

[9] Rossari F, Birocchi F, Naldini L, Coltella N. Gene-based delivery of immune-activating cytokines for cancer treatment. Trends in Molecular Medicine. 2023; 29: 329–342. https://doi.org/10.1016/j.molmed.2023.01.006

[10] Gamboa CM, Jara K, Pamarthy S, Liu L, Aiken R, Xiong Z, et al. Generation of glioblastoma patient-derived organoids and mouse brain orthotopic xenografts for drug screening. STAR Protocols. 2021; 2: 100345. https://doi.org/10.1016/j.xpro.2021.100345

[11] Dobosy JR, Rose SD, Beltz KR, Rupp SM, Powers KM, Behlke MA, et al. RNase H-dependent PCR (rhPCR): improved specificity and single nucleotide polymorphism detection using blocked cleavable primers. BMC Biotechnology. 2011; 11: 80. https://doi.org/10.1186/1472-6750-11-80

[12] Enciu AM, Codrici E, Popescu ID, Albulescu L, Dudau M, Costache I, et al. 90P Dextran-based polymers can be used as first choice to generate tumor spheroids in vitro. Annals of Oncology. 2022; 33: S1411. https://doi.org/10.1016/j.annonc.2022.09.091

[13] McCoy MG, Nyanyo D, Hung CK, Goerger JP, R. Zipfel W, Williams RM, et al. Endothelial cells promote 3D invasion of GBM by IL-8-dependent induction of cancer stem cell properties. Scientific Reports. 2019; 9: 9069. https://doi.org/10.1038/s41598-019-45535-y

[14] Shah N, Hallur PM, Ganesh RA, Sonpatki P, Naik D, Chandrachari KP, et al. Gelatin methacrylate hydrogels culture model for glioblastoma cells enriches for mesenchymal-like state and models interactions with immune cells. Scientific Reports. 2021; 11: 17727. https://doi.org/10.1038/s41598-021-97059-z

[15] Park J, Koh I, Cha J, Oh Y, Shim JK, Kim H, et al. Comparison of Glioblastoma Cell Culture Platforms Based on Transcriptional Similarity with Paired Tissue. Pharmaceuticals (Basel, Switzerland). 2024; 17: 529. https://doi.org/10.3390/ph17040529

[16] Majc B, Habič A, Malavolta M, Vittori M, Porčnik A, Bošnjak R, et al. Patient-derived tumor organoids mimic treatment-induced DNA damage response in glioblastoma. iscience. 2024; 27: 110604. https://doi.org/10.1016/j.isci.2024.110604

[17] Lindemann C, Marschall V, Weigert A, Klingebiel T, Fulda S. Smac Mimetic-Induced Upregulation of CCL2/MCP-1 Triggers Migration and Invasion of Glioblastoma Cells and Influences the Tumor Microenvironment in a Paracrine Manner. Neoplasia (New York, N.Y.). 2015; 17: 481–489. https://doi.org/10.1016/j.neo.2015.05.002

[18] Migliorini E, Thakar D, Kühnle J, Sadir R, Dyer DP, Li Y, et al. Cytokines and growth factors cross-link heparan sulfate. Open Biology. 2015; 5: 150046. https://doi.org/10.1098/rsob.150046

[19] Fujita M, Ishihara M, Ono K, Hattori H, Kurita A, Shimizu M, et al. Adsorption of inflammatory cytokines using a heparin-coated extracorporeal circuit. Artificial Organs. 2002; 26: 1020–1025. https://doi.org/10.1046/j.1525-1594.2002.07017.x

[20] Na MK, Oh Y, Lee D, Park J, Yoon SJ, Yoo J, et al. Comparison of the biological characteristics of glioblastoma tumorspheres obtained from fresh and cryopreserved glioblastoma tissues. Journal of Neuro-Oncology. 2025; 174: 191–206. https://doi.org/10.1007/s11060-025-05052-7

[21] Zhang Y, Shao Y, Li Y, Li X, Zhang X, E Q, et al. The generation of glioma organoids and the comparison of two culture methods. Cancer Medicine. 2024; 13: e7081. https://doi.org/10.1002/cam4.7081

[22] Singh SK, Abbas S, Saxena AK, Tiwari S, Sharma LK, Tiwari M. Critical role of three-dimensional tumorsphere size on experimental outcome. BioTechniques. 2020; 69: 333–338. https://doi.org/10.2144/btn-2020-0081